Revista Mexicana de Astronomía y Astrofísica, **42**, 261–272 (2006)

MULTIFREQUENCY STUDY OF THE BLUE COMPACT DWARF HARO 2: NIR IMAGING AND OPTICAL SPECTROSCOPY

H. Bravo-Alfaro,[1] R. Coziol,[1] and E. Brinks[2]

Received 2005 August 17; accepted 2006 June 14

RESUMEN

Presentamos imágenes J y H de Haro 2, las cuales confirman que el índice J-H es típico de una galaxia S0 ligeramente azul. La ausencia de asimetrías en el NIR de la zona central es similar a lo observado en galaxias tempranas a pesar de ser una galaxia rica en gas (tanto H I como CO) y de tener una elevada tasa de formación estelar. Con el fin de entender mejor esta peculiar galaxia, obtuvimos espectros ópticos de mediana resolución, los cuales sugieren formación estelar continua durante más de 10^8 años. Esta edad para el brote es consistente con la abundancia de oxígeno y con el cociente nitrógeno a oxígeno. Reanalizamos datos H I del VLA, que comparados con el NIR y con mapas de CO(1–0) confirman un evento de importante acreción de gas, probablemente mediante una interacción con una galaxia rica en gas. Nuestras observaciones indican que Haro 2 es una enana elíptica que sufrió una interacción indirecta hace más de 10^8 años, lo que produjo la acreción de una gran cantidad de gas y el subsecuente brote de formación estelar.

ABSTRACT

We carried out near infrared (NIR) imaging of the BCD Haro 2 in J and H bands which confirms that the J-H color is typical of a slightly blue S0 galaxy. The absence of asymmetries in the central NIR light distribution is similar to what is seen in unperturbed early-type galaxies, in spite of being a gas rich galaxy (in both H I and CO), with a high SFR. To better understand this peculiar object we obtained medium-resolution optical spectroscopy, which suggests continuous star formation over the past few $\times 10^8$ yr. This age for the burst is consistent with the observed oxygen abundance and with the nitrogen to oxygen ratio. We reanalyze VLA H I data which, compared with the NIR images and CO(1–0) maps, confirm a major gas accretion event, most likely the result of an interaction with a gas rich companion. Our observations indicate that Haro 2 is likely a dwarf elliptical which suffered a fly-by interaction a few times 10^8 years ago; this resulted in the accretion of a substantial amount of gas and the subsequent triggering of star formation.

Key Words: **GALAXIES: DWARF — GALAXIES: INDIVIDUAL (HARO 2) — GALAXIES: KINEMATICS AND DYNAMICS — TECHNIQUES: SPECTROSCOPIC**

1. INTRODUCTION

Blue Compact Dwarf Galaxies (BCD) are low-luminosity, low-mass, gas-rich systems, which are experiencing an active phase of star formation. Many of them share morphological and spectral properties with giant H II regions, and in the standard diagnostic diagrams used to classify emission-line galaxies, they form the high-excitation, low-metallicity branch of the starburst family. During the past two decades BCDs have been heralded as being key objects for understanding several fundamental problems in galaxy formation and evolution. However, despite many studies, several important questions remain open such as: what provides the triggering mechanisms underlying the bursts of star formation, or what lies at the origin of the different types of BCDs that can be distinguished observationally.

[1]Departamento de Astronomía, Universidad de Guanajuato, Guanjuato, México.

[2]Centre for Astrophysics Research, University of Hertfordshire, United Kingdom.

With the aim to contribute to answer these questions and, in general, to better understand the nature of different types of BCD, we decided to revisit the galaxy Haro 2 (Mkn 33, UGC 5720), providing supplementary optical and NIR observations to the wealth of observational data which has recently been accumulated on this object, with the hope of elucidating the nature of this enigmatic object.

Several groups have observed Haro 2 in recent years, but almost always as part of a larger sample of BCDs or actively star forming galaxies. Among the recent papers in which Haro 2 is mentioned is that by Chandar, Leitherer, & Tremonti (2004), presenting *HST STIS* UV spectroscopy of local starburst galaxies with an emphasis on their Wolf-Rayet (WR) content; also, in a series of papers by Cairós et al. (2001;2003) and Caón et al. (2005), optical ($BVRI$) and NIR (JHK') surface photometry of a sample of BCDs is used to study the low surface brightness stellar component; Coziol, Doyon, & Demers (2001) presented NIR spectroscopy of starburst galaxies; and Kong and his collaborators, in a series of papers, deal with a spectroscopic study at optical wavelengths of BCDs (Kong et al. 2002; Kong 2004; Shi et al. 2005). Petrosian et al. (2002) obtained an atlas of Hα, [O III], [S II] emission-line intensity distributions and Hα velocity fields of 18 BCDs, including Haro 2. Finally, Haro 2 has been the sole object of study in papers dealing with its X-ray properties (Summers, Stevens, & Strickland 2001) and its radio continuum characteristics (Beck, Turner, & Kovo 2000); this galaxy has a heavy element abundance, relative to other BCD's, of about 0.6 $Z_\odot$ (using the latest determination of $Z_\odot$ by Asplund, Grevesse, & Sauval 2005) which is fairly high for a BCD. Consequently, attempts to detect CO emission were successful and it is one of few BCDs which has CO(1–0), CO(2–1), and CO(3–2) detections (Fritz 2000; Meier et al. 2001; Israel 2005).

In a previous article (Bravo-Alfaro et al. 2004; hereafter Paper I), we presented an analysis of the kinematics of Haro 2, based on Very Large Array (VLA) H I imaging, and Owens Valley Radio Observatory (OVRO) millimeter array mapping of the CO(1–0) distribution. Table 1 summarizes the optical properties of Haro 2 as well as the results of our OVRO and VLA observations (for further details see Paper I). One of the most significant results of our analysis of the kinematics of Haro 2 (Paper I) was the discovery that the kinematical major axis of both the atomic and molecular hydrogen lies almost perpendicular to the photometric major axis. This observation was interpreted as evidence for accretion of gas, possibly due to a merger or as a result of an interaction with a gas rich companion. Assuming that the gas is of external origin also fits in with the claim, based on its light profile as first put forward by Loose & Thuan (1986), that Haro 2 is a dwarf elliptical galaxy. Haro 2 has frequently been considered to be a typical BCD. However, the main results of Paper I seem to argue against Haro 2 being a regular dIrr or LSB galaxy undergoing a starburst.

TABLE 1

OBSERVATIONAL PARAMETERS OF HARO 2

α(J2000)	$10^h\ 32^m\ 31^s.9$
δ(J2000)	$54^\circ\ 24'\ 03''$
Morph. Type	H II Im pec
M_B	-18.1
D	19.5 Mpc ($H_0 = 75\,\mathrm{km\,s^{-1}\,Mpc^{-1}}$)
v_{Hel}(HI)	1443 km s^{-1}
Δv_{50}	111 km s^{-1}
$M_{\rm H\ I}$	$2.3 \times 10^8\ M_\odot$
$M_{\rm H2}$	$0.7 \times 10^8\ M_\odot$

The finding, by many authors and for large samples of BCDs, that their optical surface brightness profiles can as often be fit by exponential as well as non-exponential ones (e.g., Caón et al. 2005 and references therein), confirm that we are dealing with a rather heterogeneous class of galaxies. In the last few years special efforts were devoted to classify different types of BCDs. For example, Cairós et al. (2001) distinguished four types of BCDs based on the morphology of the star forming regions. From a kinematical point of view, Petrosian et al. (2002), using Hα kinematical properties of 18 BCDs, separated galaxies with ordered rotational patterns from those lacking them. They confirmed that ionized hydrogen shares the peculiar kinematics seen in Haro 2 in H I and CO(1–0), and found a similar behavior in three other BCDs in their sample. This seems to confirm that decoupling between gas and stellar kinematics is relatively common, defining a class of BCDs by itself. Along the same line, Noeske et al. (2000) studied two "cometary" BCDs and Thomas et al. (2006) discovered a counter-rotating core in a dwarf elliptical (VCC 510), and concluded that a previous merger or gas accretion accompanied by star formation provided the most adequate description of this system. This all goes to show how important it is to study both the extended low surface brightness component and the central region of BCDs, in order to fully understand their evolutionary state.

In this article we continue our study of Haro 2 by presenting new images of the central region of this object in the NIR J and H bands, as well as medium-resolution optical spectroscopy. In addition, we reanalyze our H I data in order to reach a slightly higher resolution than in Paper I, so as to carry out a more detailed comparison between the gas and the old stellar components. We attempt to paint a coherent global picture of this galaxy and to investigate the triggering mechanism which lies behind the current burst of star formation. We organize this paper as follows: in § 2 we describe our NIR imaging and the optical spectroscopy. Our results are presented in § 3. In § 4 we discuss the possible origin of the H I component of Haro 2, and build a coherent picture of its star formation history, combining the results across the electromagnetic spectrum. Our conclusions are summarized in § 5.

2. OBSERVATIONS AND DATA REDUCTION

2.1. *NIR Imaging*

The NIR observations were carried out on the 7$^{\rm th}$ of April, 2002 at the 2.12 m telescope of San Pedro Mártir in Baja California, México. The images were obtained with the NIR Camera CAMILA, which consists of a NICMOS3 detector of 256×256 pixels, and which is sensitive from 1 to 2.5 μm. The optical system consists of a mirror and a focal reducer designed for the f/4.5 secondary, yielding a 3.6×3.6 arcmin^2 field of view (and corresponding to a plate scale of $0.85''$ per pixel.) Conditions were photometric and the seeing was evaluated at the telescope to be 1.1 and 0.9 arcsec in J and H, respectively.

Images in J (1.275 μm) and H (1.672 μm) were taken with total exposure times of 2800 and 1680 seconds, respectively. The observing procedure was the following. To avoid saturation of the detector, 5 exposures (co-adds) of 20 seconds integration time each were added together to form one image of 100 seconds in J. Similarly in H, 8 exposures (co-adds) of 5 seconds integration time each were added together to form one image of 40 seconds. The total integration time was obtained by adding 28 images (of 100 seconds) in J and 42 (of 40 seconds) in H, respectively.

For the flux calibration, we observed 4 standard stars from the on-line UKIRT Faint Infrared Standard Stars catalogue (http://www.mpia-hd.mpg.de /IRCAM/FAINTSTD/faintstd_1950.html): FS14, FS18, FS21, and FS24, the latter being dropped from the calibration as it turns out to be a δ Scuti variable (see Hawarden et al. 2001). The reduction and flux calibration were done using standard routines in IRAF[3]. Due to the high background levels in the NIR a somewhat more involved procedure is needed than the one usually applied in the optical. In order to determine the sky contribution, the telescope was stepped (automatically) between each image through a sequence mapping out a regular pattern, thus causing the target to fall on different areas of the detector. Because of the relatively large size of the CCD, compared to the dimension of the observed galaxy, this mosaic technique allows determination of the sky background while continuously integrating on the object. To remove short-term time variability in the sky conditions we calculated a median sky image for each sequence, using only the images within one sequence. These median images were subtracted from each individual image within their corresponding sequence. The corrected images were trimmed and the object was moved to the same reference pixel. A combined (median) image was finally obtained.

The instrument magnitudes for the standard stars were obtained using the PHOT package. Calibration equations were calculated by fitting linear regressions to the observations (neglecting the color term), using the average atmospheric extinction coefficients for San Pedro Mártir, as previously determined by Tapia, Neri, & Roth (1986). The estimated error in the calibration is $\pm$ 0.1 in both J and H.

To validate our calibration, we compare the asymptotic magnitudes, obtained by fitting standard growth curves and using circular apertures with a maximum radius of $\sim 14''$, with those of 2MASS as listed in NED (the NASA/IPAC Extragalactic Database) for a similar aperture. We find our magnitudes, $J = 11.9 \pm 0.1$ and $H = 11.27 \pm 0.1$, to be in agreement within $2\,\sigma$ with those of 2MASS, J(14 arcsec aperture) $= 12.126 \pm 0.017$ and H(14 arcsec aperture) $= 11.504 \pm 0.019$. Our $J - H = 0.63$ color as well as the colors derived on the basis of 2MASS, $J - H = 0.64$ and $H - K = 0.26$, are compatible with Haro 2 being a typical BCD, or a slightly blue S0 galaxy (according to Figure 1 in Thuan 1983).

2.2. *Optical Spectra*

Two long-slit spectra were obtained on the 9$^{\rm th}$ of May, 2002 at the 2.12 m telescope located on San Pedro Mártir. The Boller & Chivens spectrograph used in conjunction with a SITEe1024 $\times$ 1024 CCD gave

[3]IRAF (Image Reduction and Analysis Facility) is distributed by the National Optical Astronomy Observatory, which is operated by the Association of Universities for Research in Astronomy, Inc., under cooperative agreement with the National Science Foundation.

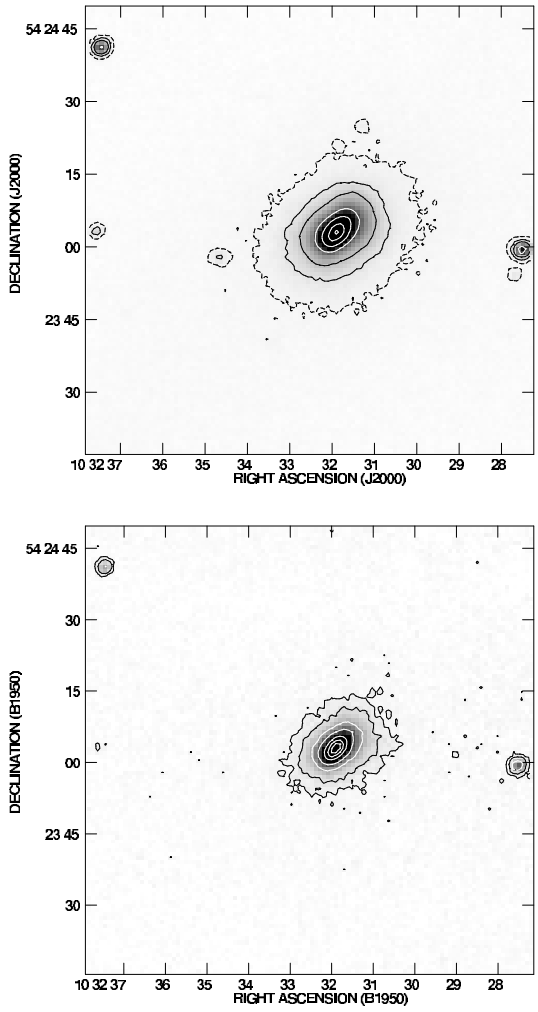

Fig. 1. NIR images of Haro 2 in both contours and grey scales, for the J (top), and H (bottom) bands.

a plate scale of 1.05″ per pixel. During the observations, the slit was opened to 240 μm, corresponding to 3.1″ on the sky. The effective seeing as estimated at the telescope was 2.3″. We used a 300 l/mm grating, blazed at 5000 Å. With the adopted slit width this yields an average resolution of 8 Å over a 4096 Å range. Due to the low sensitivity of the CCD in the blue, after reduction and flux calibration this range reduces to effectively 3500 Å.

The observations were performed under low airmass conditions so as to minimize differential diffraction. The effective airmass was 1.09. We took three spectra of 900 s exposure time each with the slit aligned in the E–W direction, and three further spectra with the slit aligned along the major axis of the galaxy (135°). The E–W spectra, which are less susceptible to guiding errors, were used to verify if two

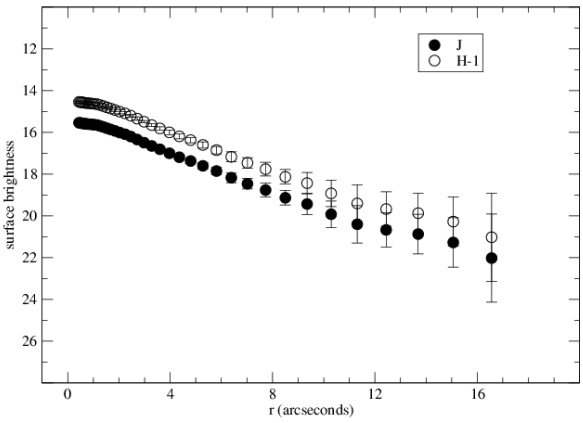

Fig. 2. Surface brightness profiles in J and H. The H isophotes were shifted by −1 mag for clarity.

of the bright objects near Haro 2 and aligned along that axis were of stellar origin. However, we did not reach a high enough S/N to arrive at any conclusion on this issue. A He–Ar lamp was used for wavelength calibration and three standard stars were observed to flux-calibrate the spectra. A few cirrus clouds observed at the end of the night suggest that conditions were not photometric.

Standard procedures for the reduction of long-slit spectra were followed using IRAF. For each of the two position angles, emission features were measured separately in the three spectra using the Gaussian fitting tool in SPLOT. A mean variation of 13% was observed for the fluxes. Part of this variation reflects changes in sky condition during the observation, including effects due to differential refraction. A mean variation of only 4% was observed for the equivalent width in different spectra. For each of the two position angles, an average spectrum was obtained by combining the three 1-dimensional spectra of 900 s each. The final fluxes are those measured in the combined spectra. The adopted estimated errors are 13% and 4% for the fluxes and equivalent widths, respectively.

3. RESULTS

3.1. *NIR Imaging Analysis*

The main goal of our NIR imaging analysis is to check for possible counterparts of the kinematical peculiarities observed in H I and CO, and check if a recent, strong interaction or merger could lie at their origin. According to simulations of interacting/merging galaxies (Iono, Yun, & Mihos 2004; Mihos & Hernquist 1996; Hernquist & Mihos 1995), such events should lead to a substantial perturbation of the stellar morphology dominated by an $m = 2$ or

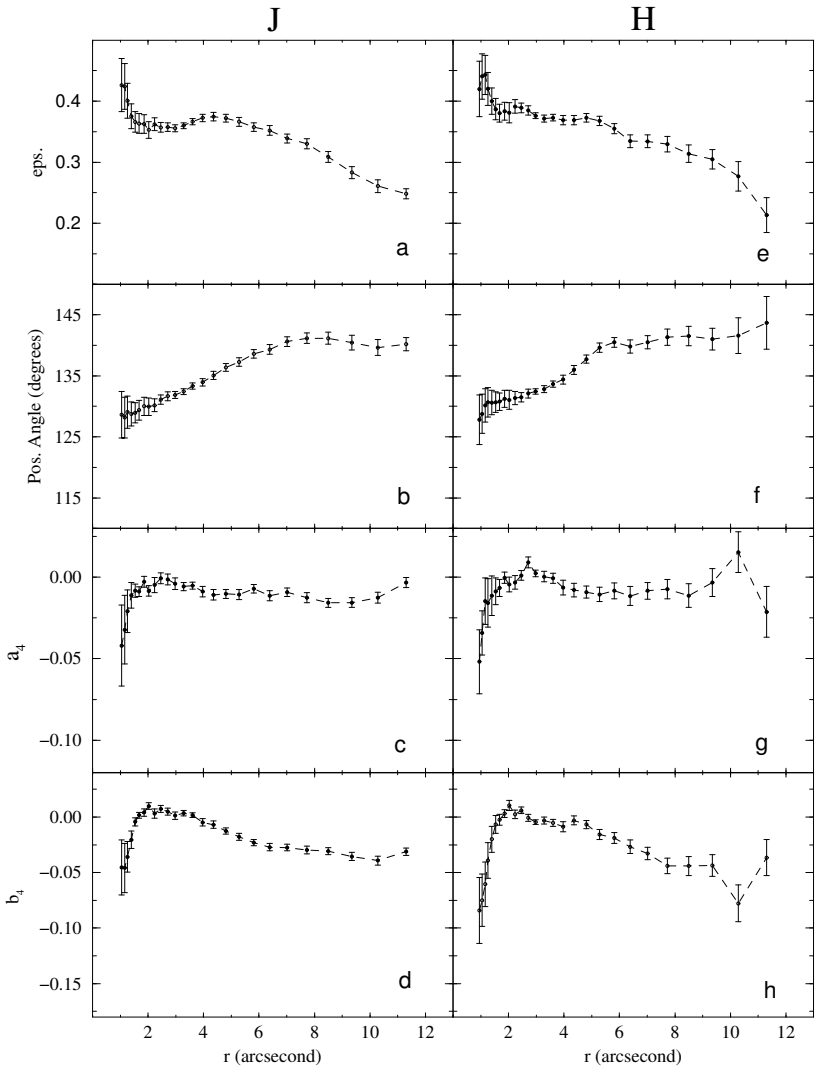

Fig. 3. Variation of the ellipse fitting parameters as a function of radius: ellipticity (a and e); Position Angle (b and f); first harmonic a_4 (c and g); and second harmonic b_4 (d and h).

bar-like structure. Our images in J and H are presented in Figure 1. These images are sensitive to the most luminous (inner) part of the galaxy, reaching surface brightnesses of ~ 22 mag arcsec^{-2} in J and ~ 21 mag arcsec^{-2} in H. On first inspection, our images show no obvious perturbation in the inner part of the galaxy.

We obtained surface brightness profiles and integrated magnitudes in order to compare our observations with previous surveys. Profiles of the inner regions of Haro 2 in J and H were obtained by fitting elliptical isophotes. The fitting procedure was carried out using the package ELLIPSE within IRAF (Busko 1996). The resulting profiles for J and H are shown in Figure 2. Over the range $1''$ to $12''$ our profiles agree with those found by Cairós et al. (2003), except for a slight systematic shift, our measurements being ~ 0.15 magnitudes brighter. This, by the way, goes in the same direction as the comparison of our integrated magnitudes with those given by 2MASS, suggesting that there is a slight 0.15 mag offset to our calibration. Within $1''$ radius our data are degraded by seeing whereas beyond $12''$ our data fall systematically below the curve published by Cairós et al. This can be traced to uncertainties in the subtraction of the sky background. For the remainder of the paper, we will restrict our analysis to the inner $12''$ in radius.

In order to quantify possible peculiarities in the old stellar population in the central regions of Haro 2

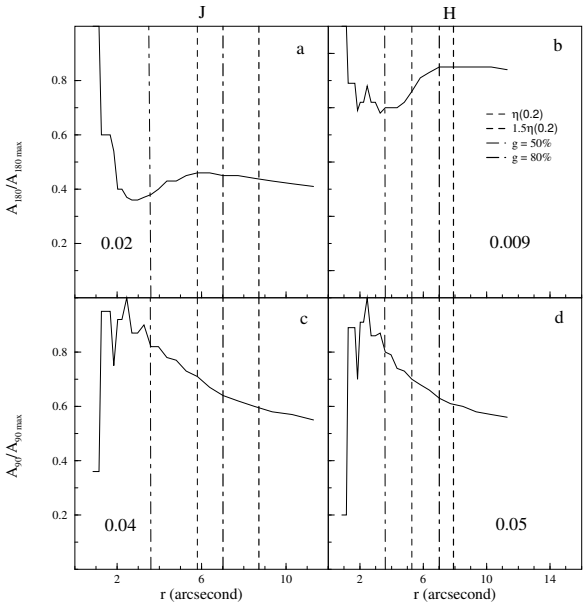

Fig. 4. Asymmetry parameters A_ϕ as a function of radius. The asymmetry is normalized by the peak value which is indicated in each panel. The four different vertical lines mark four reference radii, as defined in CBJ. Values of the asymmetry at each radius are given in Table 2.

we apply two independent methods. First we fitted ellipses to the isophotes of the J and H images. The isophotal fits give information on the variation of ellipticity (*eps*), the variation of position angle of the major axis and on the deviations of the isophotes from a perfect ellipse (as described by the harmonics a_4 and b_4; Barth, Coziol, & Demers 1995, and references therein). In Figure 3 it can be seen that the variations of the parameters in J and H are nearly identical. This suggests that the two colors trace the distribution of the same stellar population, dust not being important at these wavelengths.

In Fig. 3 (a) and (e), the isophotes are seen to become rounder towards large radii. This variation is accompanied by a small increase in position angle in Fig. 3 (b) and (f). The small variations observed for the ellipticity and position angle are typical of a homogeneous mass distribution. The low values of a_4 indicate only a small deviation from a perfect ellipse, while the low values of b_4 indicate a near perfect alignment with the semi major axis. The negative value for a_4 suggests a marginally boxy isophote. All these parameters are typical of an evolved bulge or a normal, unperturbed early-type galaxy (E or S0).

To double check our analysis, we have also determined the level of asymmetry of the central region

TABLE 2

VALUES OF THE ASYMMETRY AT FOUR DIFFERENT RADII AS DEFINED IN CBJ

		J		H	
	r (arcsec)	A_{180}	A_{90}	A_{180}	A_{90}
$\eta(0.2)$	5.8	0.008	0.028	0.007	0.031
$1.5\eta(0.2)$	8.7	0.007	0.024	0.007	0.027
g(50)	3.6	0.006	0.033	0.006	0.036
g(80)	7.0	0.008	0.026	0.007	0.029

of the galaxy. The asymmetry A_ϕ of an image is a quantitative parameter based on comparing a source image with its image rotated by an angle ϕ. We defined A_ϕ following Conselice, Bershady, & Jangren 2000 (hereafter CBJ) as $A_\phi^2 = \sum(I_0 - I_\phi)^2 / 2\sum I_0^2$, where I_0 is the intensity distribution in the original image and I_ϕ is the intensity distribution in the image rotated by an angle ϕ. In Figure 4 we present the results for the angle $\phi = 180$ and $\phi = 90$, as determined in the two filters J and H. The values of A_ϕ are normalized by their peak value (indicated within each figure).

The forms of the different plots for the two filters are remarkably similar, confirming that the two filters are mapping the same stellar population. In Table 2 we give the values of A_ϕ for four different radii, as defined by CBJ. Compared to the results obtained by these authors in the R band, we find a behavior similar to that of normal, unperturbed early-type galaxies (E/S0): very low values of A_ϕ, with a maximum in the center, decreasing towards the edge.

Our analysis in the central region of Haro 2 agrees and complements the morphological analysis previously made by Loose & Thuan (1986) and by Cairós et al. (2003); both observed smooth intensity drops over the entire radius range covered by their different filter images (up to 50″). Based on the morphological analysis, we conclude that there is no evidence of any asymmetries in the stellar population over the studied area. As we will see in the discussion, this sets constraints on the kind of event which could have caused the recent accretion of gas in this galaxy.

3.2. *Optical Spectrum*

We obtained medium resolution spectra at two different slit positions; one along the major axis (135°), and a second one along the E–W direction. Figure 5 shows a section of the observed 2-D spec-

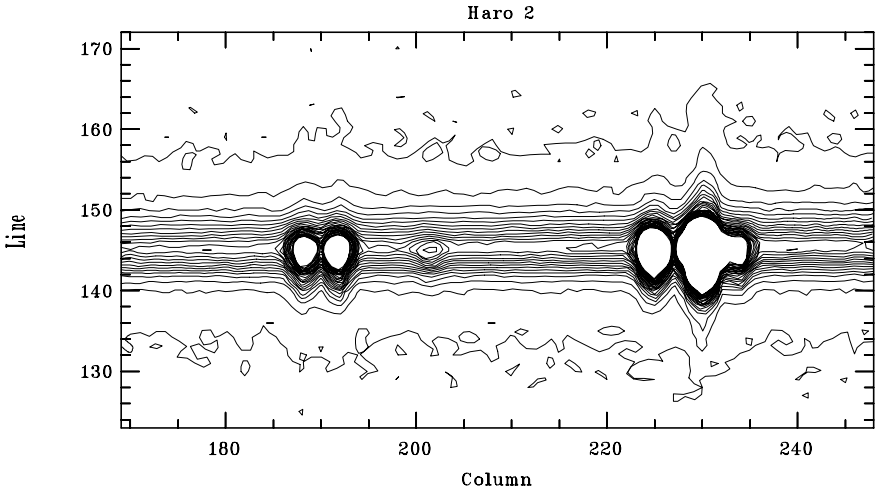

Fig. 5. Section of the 2-D spectrum for the slit positioned at 135°. The plate scale per pixel corresponds to 1.05″ (rows) and 4 Å (columns), respectively. The emission lines that are visible near column 190 are the two sulfur lines [S II]$\lambda\lambda$6716,6731; Hα is seen near column 230, bracketed by the two nitrogen lines, [N II]$\lambda\lambda$6548,6584.

trum for the slit at an orientation of 135°. The emission lines seen there are: the two sulfur lines [S II]$\lambda\lambda$6731,6717 Å, Hα at λ6563 Å, and the two lines of [N II]$\lambda\lambda$6548,6584 Å. The emission related to the ionized region is more intense in the center of the galaxy. The region of highest intensity covers 13″. A similar distribution is observed for the E–W slit orientation, in which case the ionized region covers 10″. Adopting a distance of 19.5 Mpc (see Table 1), this corresponds to linear extents of 1.2 and 1.0 kpc for the 135° and E–W orientations, respectively. Note that ionized gas occupies the inner 1/3 of our NIR images. The extent of the active zone, as seen by our spectra, coincides with the region where we detect CO(1–0) and where the gas column density exceeds the threshold above which it becomes gravitationally unstable (see Paper I).

The fully reduced (1–D) spectrum for the 135° slit orientation, shifted to the rest frame, is presented in Figure 6. The aperture used to reduce the 2–D spectra to 1–D was 15 pixels wide. The E–W spectrum is very similar. Both spectra show strong emission lines and a continuum which is rising towards the blue (the drop blueward of 4000 Å is an artifact which has not been calibrated out entirely). In both spectra we note a weak bump blueward of Hβ. This part of the spectrum is shown enlarged in Figure 7. This is the telltale He II λ4686 line, typical of WR stars, the presence of which implies a current phase of star formation (Kunth & Joubert 1985; Conti 1991; Guseva, Izotov, & Thuan 2000).

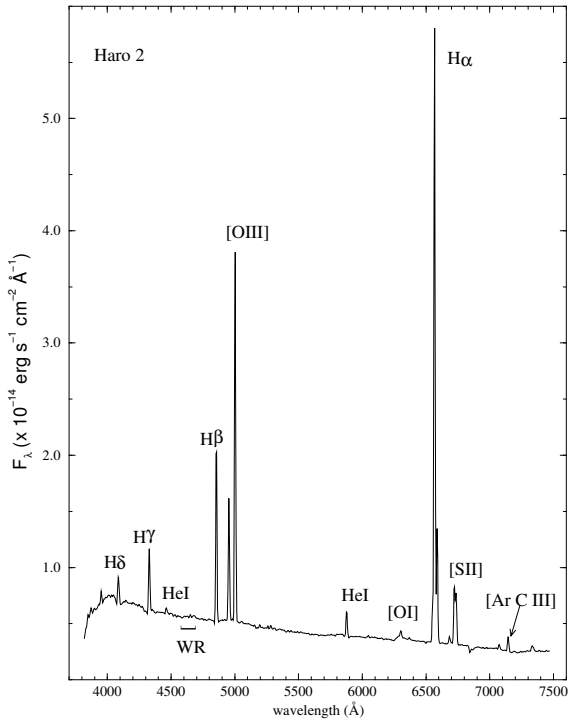

Fig. 6. 1–D spectrum for the slit aligned at 135°. The spectrum oriented E–W is very similar.

Fluxes before (F_{raw}) and after (F_λ) correction by extinction, and equivalent widths (W_λ) for the most important lines are reported in Table 3. The fluxes for the Balmer lines were corrected for an amount of

TABLE 3

LINE FLUXES AND EQUIVALENT WIDTHS OF THE BRIGHTEST EMISSION LINES

Line	λ	(E–W)			(135°)		
		$F_{raw} \times 10^{-13}$	$F_\lambda \times 10^{-13}$	W_λ	$F_{raw} \times 10^{-13}$	$F_\lambda \times 10^{-13}$	W_λ
	Å	(erg cm^{-2} s^{-1})	(erg cm^{-2} s^{-1})	Å	(erg cm^{-2} s^{-1})	(erg cm^{-2} s^{-1})	Å
Hβ	4861	1.66	2.80	43.31	2.62	4.04	39.03
[O III]	4959	1.17	1.78	29.15	1.52	2.31	23.43
[O III]	5007	3.61	5.47	91.12	4.59	6.96	69.43
[N II]	6548	0.28	3.78	10.66	0.38	5.13	9.62
Hα	6563	5.83	7.98	220.7	8.30	11.2	202.4
[N II]	6583	0.98	1.32	37.23	1.49	2.00	36.28

4 Å of absorption (which is the appropriate value for A type stars), using the following expression:

$$F_\lambda^{corr} = F_\lambda^{obs}(1 - \frac{W_\lambda^{abs}}{W_\lambda^{obs}}) .$$

The Balmer equivalent widths were corrected by:

$$W_\lambda^{corr} = W_\lambda^{obs} - W_\lambda^{abs}.$$

All fluxes were corrected for dust extinction due to the Galaxy and for internal extinction. We assumed Case B Balmer decrements and the reddening curve parameterized by Miller & Mathews (1972). We find total values of $c_{H\beta}^{obs} = 0.30$ and 0.34 for the 135° and E–W slits, respectively. To find the contribution by Galactic extinction we used E(B–V)= 0.12 (based on Schlegel, Finkbeiner, & Davis 1998) to find $c_{H\beta}^{int} = c_{H\beta}^{obs} - 1.45\mathrm{E(B–V)} = c_{H\beta}^{obs} - 0.17$. This yields $c_{H\beta}^{int} = 0.13$ and 0.17 for the 135° and E–W slit orientations. The fluxes, both before and after the extinction correction, as well as the reported equivalent widths, are in general agreement with those published by Kong et al. (2002); any differences can be ascribed to the slits having sampled slightly different parts of the star burst region.

The strong Balmer absorption features observed in our spectra (see Fig. 7) have been previously reported by Mas-Hesse & Kunth (1999), and are indicative of the presence of a population of intermediate mass, A-type stars (Rose 1985). According to Charlot & Bruzual (1991), the contribution of such stars to the total stellar population of an instantaneous burst of star formation becomes important ~ 0.4 Gyr after the start of a burst. The presence of these stars together with WR stars may suggest continuous star formation; or alternatively, these stars could be the products of previous bursts of star formation. However, as we discuss below, the presence of the A-type population is not a sufficient criterion to compute the age of the burst, in part because these galaxies are known to harbor age-composite stellar populations (see e.g., Raimann et al. 2000).

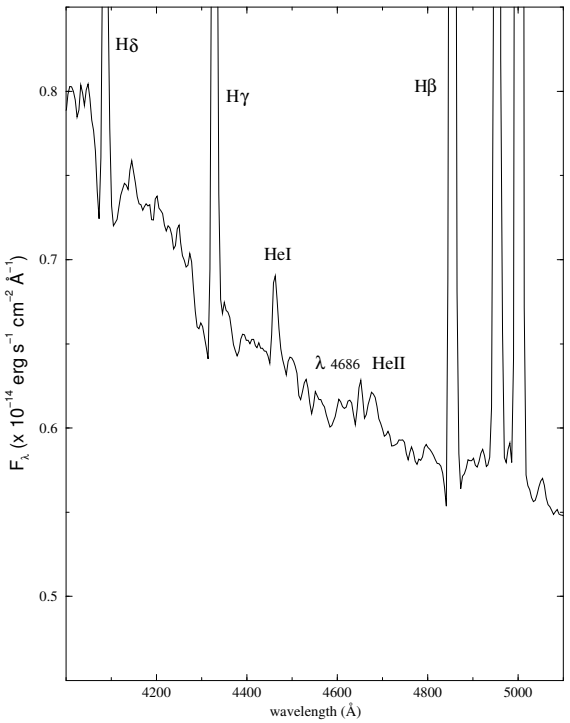

Fig. 7. Enlargement of the region around the WR feature. The He II line at λ4686 can be clearly seen. Balmer absorption is also evident, signaling the presence of a significant population of intermediate (A-type) stars.

For an assumed distance of 19.5 Mpc, the luminosity in Hα is $\log(L_{H\alpha})$= 40.7 erg s^{-1} (or 40.6 erg s^{-1} in the E–W spectrum). According to Kennicutt (1983) this yields a present star formation rate of SFR($>$ 10 $M_\odot$) = 0.07 $M_\odot$ yr^{-1} and a total

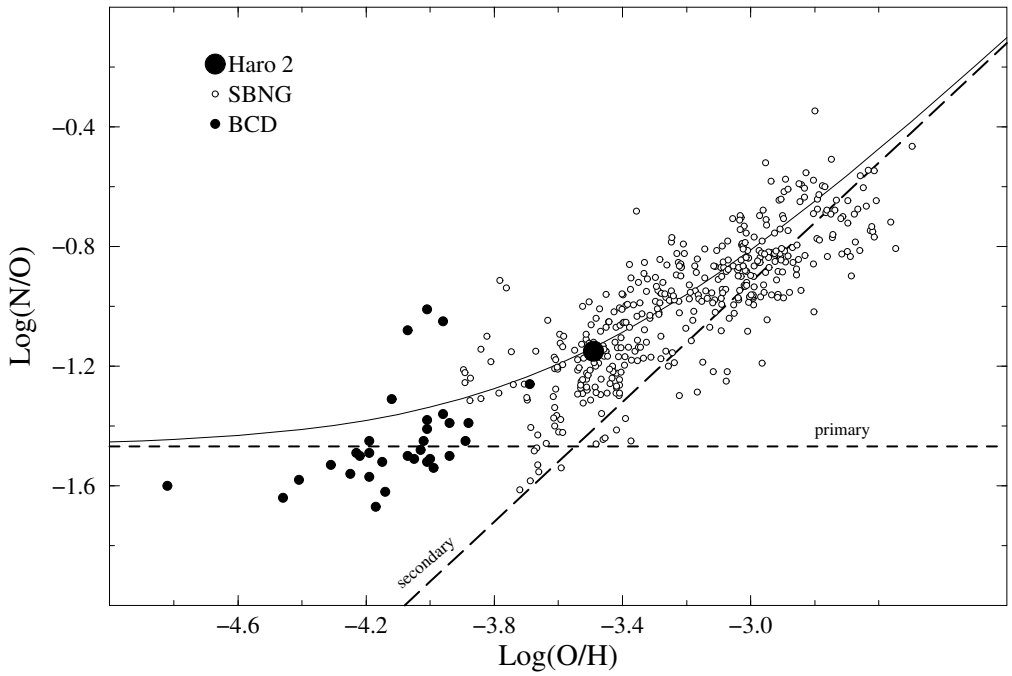

Fig. 8. Abundance of N/O as a function of O/H. The continuous line is a model of Primary + Secondary origin for the gas (Vila-Costas & Edmunds 1993). In Haro 2, the values of N/O and O/H suggest a secondary contribution, consistent with a burst age greater than 10^8 yr.

star formation rate of SFR(total) = 0.5 $M_\odot$ yr^{-1}. From the E–W spectrum we get SFR($>$ 10 $M_\odot$) = 0.05 $M_\odot$ yr^{-1}, and SFR(total) = 0.3 $M_\odot$ yr^{-1}. Given the current supply in the form of atomic and molecular hydrogen, these star formation rates could be sustained over some 10^9 yr.

The oxygen abundance, O/H, and the nitrogen to oxygen ratio, N/O, were estimated using the methods developed by Thurston, Edmund, & Henry (1996). Uncertainties adopted for these values are 0.2 dex for log(O/H) and 0.1 dex for log(N/O). For the oxygen abundance we find a value of 12 + log(O/H)= 8.5, in good agreement with the value of 8.4 reported by Chandar et al. (2004) and Kong (2004), and with the metallicity reported by Mas-Hesse & Kunth (1999). This is relatively high for a BCD. The same is also true for N/O which we find to be log(N/O)= −1.2 (the two slit orientations yield the same values). Such relatively high values make Haro 2 a more evolved galaxy as compared to typical BCD's. Figure 8 shows where Haro 2 is located on a diagram of N/O as a function of O/H. The continuous line indicates a model for *Primary + Secondary* origin for nitrogen (Vila-Costas & Edmunds 1993). The abundances found in Haro 2 are consistent with a secondary origin for nitrogen.

Given that we know the metallicity and the equivalent width in Hα, we can estimate the age of the last burst using the Starburst'99 model (Leitherer et al. 1999). With a metallicity $Z = 0.008$ and a maximum log(EW$_{\rm H\alpha}$) of 2.34 Å, we find two possible results: for an instantaneous burst, we get an age of 5.4×10^6 yr. On the other hand, if we assume continuous star formation with a Salpeter IMF, and an upper mass limit of 100 $M_\odot$, the data yield an age of 3.4×10^8 yr. Note that the model cannot distinguish between constant star formation and a succession of shorter bursts over the same period (Coziol et al. 2001).

4. DISCUSSION

Our NIR analysis suggests that Haro 2 is a typical dE or an abnormally blue S0 galaxy. The blue color is obviously produced by the active star formation observed in the spectra. In order to explore the relation between the active star formation and the gas history, we started out with a reanalysis of our 21 cm H I data, improving the spatial resolution by almost 20%. The resulting H I map has a beam size of $12''\times13''$, and a slight loss of sensitivity in the outermost regions of the galaxy (cf. Paper I). But this does not affect our present goals as we are mainly interested in the central region of Haro 2.

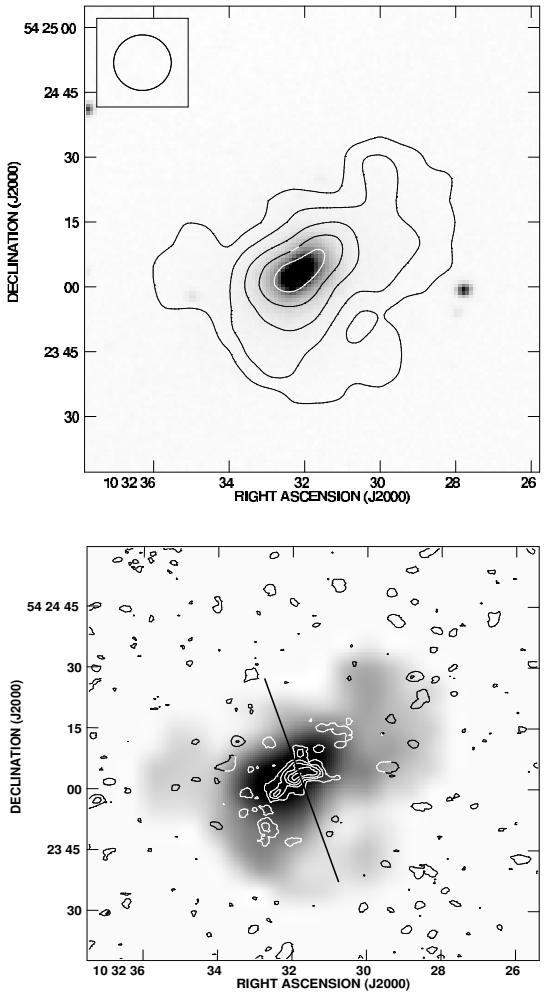

Fig. 9. Top: 21 cm H I contours superposed on the *J*-band NIR image. H I contours are 1.9, 6.3, 12.7, 19.0, and $25.3\times10^{20}\,\mathrm{cm}^{-2}$. The beam size is indicated by the circle at the upper left. Bottom: Overlay of CO(1–0) contours on the H I in grey scales. Contours are multiples of 0.52 $\mathrm{Jy\,beam}^{-1}\,\mathrm{km\,s}^{-1}$. The beam size for CO is $3.3''\times2.6''$. The line indicates the kinematical major axis (cf. Paper I).

In Figure 9 (top) we show the H I contours superposed over our J-band NIR image. The H I distribution of Haro 2 is neatly aligned with the photometric major axis, as is true for the CO emission (Fig. 9 bottom). However, as discussed in Paper I, the kinematical major axis lies nearly perpendicular to the stellar disk outlined by the optical and NIR. This particular configuration strongly suggests that a large fraction of the gas now seen in Haro 2 was recently accreted.

The reanalysis of our H I data with a slightly better resolution gives us an additional argument in support of gas accretion. The higher resolution H I map seen in Fig. 9 shows a warp-like structure developing at both NW and SE sides of Haro 2, a morphology which is reflected even in CO (Fig. 9 bottom). This indicates that the gas (atomic and molecular) has not properly settled down yet.

Regarding the origin of this H I, we explore the hypothesis that Haro 2 has interacted with and captured an intergalactic H I cloud. In the literature, some have claimed examples where galaxies could have interacted with intergalactic H I clouds, or the so called "dark" galaxies (Bouchard, Carignan, & Staveley-Smith 2006; Minchin et al. 2005; Boyce et al. 2001; Giovanelli & Haynes 1989). However, up to now, further analysis has always revealed optical counterparts to these seemingly isolated H I clouds, or has come up with circumstantial evidence for the tidal origin of such clouds (Walter, Skillman, & Brinks 2005; Oosterloo & van Gorkom 2005; Chengalur, Giovanelli, & Haynes 1995). The existence, or rather lack thereof, of such dark clouds has been neatly summarized by Briggs (2004). We therefore expect that the probability of accretion of gas from an intergalactic H I cloud for Haro 2 is rather low.

It seems obvious, however, that Haro 2 has recently ($< 10^9$ yr) accreted gas, which has triggered the star formation activity observed in this galaxy. Based on our observations in the NIR and our spectroscopy we may put some constraints on the possible origin of such events. First, using Starburst'99 models, we have found two possible solutions for the duration of the burst: a very young burst of 10^6 yr, and a longer-duration one, consistent with constant star formation over a period of 10^8 yr. Now, considering the high metallicity and abundance of nitrogen observed in Haro 2, it seems difficult to sustain the instantaneous star formation scenario. In particular, the fact that the nitrogen has a secondary origin rules out that it could be produced by the massive stars (O and/or WN stars) evidenced by the spectra.

Another problem with the instantaneous burst hypothesis is that we would need to see a companion close by, which is not observed. The absence of asymmetries and the smoothness of the NIR profiles also seem in contradiction with a violent or recent interaction event.

On the other hand, the second hypothesis of a burst duration of several times 10^8 yr, or a sequence of bursts over such period (Coziol et al. 1999; 2001) has many advantages. First, this is consistent with all the features observed in the spectra (including the Balmer absorption lines), with the high metallicity (giving enough time for self-enrichment), and

the nitrogen production by intermediate mass stars. Second, this also supports an interaction in the past ($>10^8$ yr), which would explain the smoothness of the stellar distribution and lack of asymmetry. Considering a longer time for the accretion of gas and triggering of the burst also opens the possibility of a fly-by interaction with a gas-rich galaxy located now farther away than would be expected in the instantaneous burst scenario.

In Paper I we described how the outer reaches of the H I envelope of Haro 2 are perturbed, displaying features that could well be attributed to a fly-by interaction with a putative gas-rich companion galaxy (see also Thuan, Hibbard, & Lévrier 2004). The task is then to identify this companion. Examining the nearby environment of Haro 2, we proposed in Paper I two candidates for such an event: a galaxy lying 4.7′ to the East (Huchtmeier, Sage, & Henkel 1995), at a projected distance of 27 kpc, and subsequently identified as SDSS J103300.66+542607.9, and a second one, identified as UGC 5676 (Pustilnik et al. 2001), projected to the NE from Haro 2, at a distance of 200 kpc. It turns out that the first candidate has a measured redshift of $z = 0.065$, and can be safely ruled out. The second galaxy, on the other hand, has a recession velocity of 1412 km, very close to that of Haro 2 (1443 km).

Considering the physical characteristics of UGC 5676 in more detail, we first note that it is projected to the NE from Haro 2 at a distance of 200 kpc. This galaxy, with a Hubble type SBdm, was detected in H I by Haynes & Giovanelli (1991) who reported an H I mass of 3.7×10^8 $M_\odot$, i.e., about 1.5 times more massive in H I than Haro 2. This confirms that UGC 5676 is a gas-rich galaxy, as required by our scenario. Furthermore, the optical image on the DSS plate looks highly perturbed. In a fly-by scenario, therefore, it seems conceivable that UGC 5676 has donated a fraction of its gas to Haro 2 without causing much distortion to its light distribution.

Assuming that star formation was initiated by the interaction, some 3.8×10^8 yr ago (see § 3.2), the mean spatial velocity difference between the two galaxies would need to be, at least, 500 km/s. This is quite a high velocity which would need to be even higher if the true distance between UGC 5676 and Haro 2 is larger than the projected separation. However, we should also consider that the gas expelled as a result of the fly-by would have needed quite some time to settle into the gravitational potential of the receiving galaxy, gravitate to the center, cool dynamically, and become unstable to gravitational collapse, eventually leading to the star formation witnessed in Haro 2. This means that the time elapsed since closest approach is underestimated by some unknown amount. For example, assuming the time estimate for closest approach is twice the age of the burst we estimated, namely 7.6×10^8 yr, the difference in velocity would come out to be a more comfortable 250 km s^{-1}. A somewhat longer time between closest approach and the onset of star formation also goes a long way to explaining the smoothness of the stellar distribution and for the gas to settle down (albeit in a different plane than the stars).

5. CONCLUSIONS

We have obtained NIR images in J and H and medium-resolution optical spectroscopy to further investigate the nature of the blue compact dwarf Haro 2. In addition, we have built higher resolution H I maps from data previously obtained, and compared them with the old stellar distribution, imaged in the NIR. We summarize our results as follows:

(1) We confirm the early-type morphology (dE or S0) of Haro 2. Applying independent methods of analysis on our NIR images, very smooth NIR profiles and a low level of asymmetry are found, similar to what is observed in unperturbed, early-type galaxies. The smoothness of the older stellar distribution argues against a recent, strong interaction or merger.

(2) Our optical medium-resolution spectroscopy confirms that recent star formation activity is present in Haro 2, as indicated by the presence of lines such as He II λ4686, produced by short-lived WR stars. We also note the presence of an important intermediate age stellar population.

(3) From our spectroscopy, we find the metallicity of Haro 2 to be rather high for a BCD, and the nitrogen abundance to have a secondary origin, which rules out the instantaneous star formation scenario. Using the Starburst'99 model with a Salpeter IMF and an upper mass limit of 100 $M_\odot$, we found good agreement for constant star formation (or a succession of bursts) over a period of 3.4×10^8 yr.

(4) Refining our observations in H I and comparing the gas distribution with our NIR images, we find some evidence for a slight warp in the H I and CO distributions which corroborates our preferred scenario of Haro 2 having undergone a major accretion event.

(5) Assuming that star formation started several times 10^8 years ago, we identified UGC 5676 at a projected distance of $\approx$ 200 kpc as a possible candidate that might lie at the origin of the H I gas and of the star formation activity observed in Haro 2.

We thank an anonymous referee for comments which significantly improved this article. This research has made use of the NASA/IPAC Extragalactic Database (NED), which is operated for NASA by the Jet Propulsion Laboratory, California Institute of Technology. We have also used the Digital Sky Survey, produced at the Space Telescope Science Institute. HBA and RC thank CONACyT, México, for its support through grant 40194–F.

REFERENCES

Asplund, M., Grevesse, N., & Sauval, A. J. 2005, in ASP Conf. Ser. Vol. 336, Cosmic Abundances as Records of Stellar Evolution and Nucleosynthesis in honor of David L. Lambert, eds. T. G. Barnes III & F. N. Bash (San Francisco: ASP), 25
Barth, C., Coziol, R., & Demers, S. 1995, MNRAS, 276, 1224
Beck, S. C., Turner, J. L., & Kovo, O. 2000, AJ, 120, 244
Bouchard, A., Carignan, C., & Staveley-Smith, L. 2006, AJ, in press
Boyce, P. J., Minchin, R. F., Kilborn, V. A., et al. 2001, ApJ, 560, L127
Bravo-Alfaro, H., Brinks, E., Baker, A. J., Walter, F., & Kunth, D. 2004, AJ, 127, 264 (Paper I)
Briggs, F. 2004, in IAU Symp. 217, Recyling Intergalactic and Interstellar Matter, eds. P.-A. Duc, J. Braine, & E. Brinks (San Francisco: ASP) 26
Busko, I. 1996, in ASP Conf. Ser. Vol. 101, The Fifth Astronomical Data Analysis Software and Systems Conference, eds. G. H. Jacoby & J. Barnes (San Francisco: ASP), 139
Cairós, L. M., Caón, N., Papaderos, P. Noeske, K., Vílchez, J. M., García, L. B., & Muñoz–Tuñón, C. 2003, ApJ, 593, 312
Cairós, L. M., Caón, N., Vílchez, J. M., González-Pérez, J. N., & Muñoz-Tuñón, C. 2001, ApJS, 136, 393
Caón, N., Cairós, L. M., Aguerri, A. L. & Muñoz-Tuñón, C. 2005, ApJS, 157, 218
Chandar, R., Leitherer, C., & Tremonti, C. A. 2004, ApJ, 604, 153
Charlot, S., & Bruzual, G. A. 1991, ApJ, 367, 126
Chengalur, J. N., Giovanelli, R., & Haynes, M. P. 1995, AJ, 109, 2415
Conselice, J., Bershady, M. A., & Jangren, A. 2000, ApJ, 529, 886
Conti, P. 1991, ApJ, 377, 115
Coziol, R., Doyon, R., & Demers, S. 2001, MNRAS, 325, 1081
Coziol, R., Reyes, R. E., Considère, S., Davoust, E., & Contini, T. 1999, A&A, 345, 733
Fritz, T. 2000, Ph.D. Thesis, University of Bonn
Giovanelli, R., & Haynes, M. P. 1989, ApJ, 346, L5
Guseva, N. G., Izotov, Y. I., & Thuan, T. X. 2000, ApJ, 531, 776
Hawarden, T. G., Leggett, S. K., Letawsky, M. B., Ballantyne, D. R., & Casali, M. M. 2001, MNRAS, 325, 563
Haynes, M. P. & Giovanelli, R.1991, ApJS, 77, 331
Hernquist, L. & Mihos, J. C. 1995, ApJ, 448, 41
Huchtmeier, W. K., Sage, L. J., & Henkel, C. 1995, A&A, 300, 675
Iono, D., Yun, M. S., & Mihos, C. 2004, ApJ, 616, 199
Israel, F. P. 2005, A&A, 438, 855
Kennicutt, R. C. Jr. 1983, ApJ, 272, 54
Kong, X. 2004, A&A, 425, 417
Kong, X., Cheng, F. Z., Weiss, A., & Charlot, S. 2002, A&A, 396, 503
Kunth, D., & Joubert, M. 1985, A&A, 142, 411
Leitherer, C., Schaerer, D., Goldader, J. D., et al. 1999, ApJS, 123, 3
Loose, H.-H., & Thuan, T. X. 1986, ApJ, 309, 59
Mas-Hesse, J. M., & Kunth, D. 1999, A&A, 349, 765
Meier, D. S., Turner, J. L., Crosthwaite, L. P., & Beck, S. C. 2001, AJ, 121, 740
Mihos, C. J., & Hernquist, L. 1996, ApJ, 464, 641
Miller, J. S., & Mathews, W. G. 1972, ApJ, 172, 593
Minchin, R., Davies, J., Disney, M., et al. 2005, ApJ, 622, L21
Noeske, K. G., Guseva, N. G., Fricke, K. J., Izotov, Y. I., Papaderos, P., & Thuan, T. J. 2000, A&A, 361, 33
Oosterloo, T., & van Gorkom, J. 2005, A&A, 437, L19
Petrosian, A. R., Movsessian, T., Comte, G., Kunth, D., & Dodonov, S. 2002, A&A, 391, 487
Pustilnik, S. A., Kniazev, A. Y., Lipovetsky, V. A., & Ugryumov, A. V. 2001, A&A, 373, 24
Raimann, D., Bica, E., Storchi-Bergmann, T., Melnick, J., & Schmitt, H. 2000, MNRAS, 314, 295
Rose, J. A. 1985, AJ, 90, 1927
Schlegel, D. J., Finkbeiner, D. P., & Davis, M. 1998, ApJ, 500, 525
Shi, F., Kong, X., Li, C., & Cheng, F. Z. 2005, A&A, 437, 849
Summers, L. K., Stevens, I. R., & Strickland, D. K. 2001, MNRAS, 327, 385
Tapia, M., Neri, L., & Roth, M. 1986, RevMexAA, 13, 115
Thomas, D., Brimioulle, F., Bender, R., et al. 2006, A&A, 445L, 19
Thuan, T. X. 1983, ApJ, 268, 667
Thuan, T. X., Hibbard, J. E., & Lévrier, F. 2004, AJ, 128, 617
Thurston, T. R., Edmund, M. G., & Henry, R. B. C. 1996, MNRAS, 283, 990
Vila-Costas, M. B., & Edmunds, M. G. 1993, MNRAS, 265, 199
Walter, F., Skillman, E. D., & Brinks, E. 2005, ApJ, 627, L105

Héctor Bravo-Alfaro and Roger Coziol: Depto. de Astronomía, Universidad de Guanajuato, Apdo. Postal 144, 36000 Guanajuato, Gto., México (hector, rcoziol@astro.ugto.mx).
Elias Brinks: Centre for Astrophysics Research, University of Hertfordshire, College Lane, Hatfield AL10 9AB, U.K. (ebrinks@star.herts.ac.uk).